Title

Aqueous peptides as experimental models for hydration water dynamics near protein surfaces

Journal

Physical Chemistry Chemical Physics, 10(32)

ISSN

0956-5000

Authors

Malardier-Jugroot, Cecile
Johnson, Margaret E
Murarka, Rajesh K
et al.

Publication Date

2008

DOI

10.1039/b806995f

Peer reviewed

Dielectric Relaxation of Aqueous Solutions of Hydrophilic vs. Amphiphilic Peptides

Rajesh K. Murakra[1,†] **and Teresa Head-Gordon**[1,2,*]

Department of Bioengineering, University of California, Berkeley[1]

Physical Biosciences Division, Lawrence Berkeley National Laboratory[2]

Berkeley CA 94720

Abstract

We report on molecular dynamics simulations of the frequency-dependent dielectric relaxation spectra at room temperature for aqueous solutions of a hydrophilic peptide and an amphiphilic peptide at two concentrations. We find that only the amphiphilic peptide exhibits all of the anomalous dielectric response exhibited by aqueous protein solutions: a dielectric increment over bulk water, an imaginary part of the frequency-dependent dielectric that is bimodal at high concentration, a real part of the frequency-dependent dielectric of the high concentration peptide solution that drops precipitously and below the value for the low concentration, and two δ-relaxations at the picosecond and nanosecond timescales. We show that the molecular origin of the dielectric relaxation anomalies is due to frustration in the water network arising from the amphiphilic chemistry of the peptide that does not allow it to reorient on the picosecond timescale of bulk water motions. This explanation is consistent with the idea of "slaving" of residue side chain motions to protein surface water, and furthermore offers the possibility that the anomalous dynamics observed from a number of spectroscopies arises at the interface of hydrophobic and hydrophilic domains on the protein surface.

[†]Current address: Baker Laboratory of Chemistry and Chemical Biology, Cornell University, Ithaca, NY, 14853. *Corresponding author

INTRODUCTION

Dielectric relaxation (DR)[1-6] provides a powerful spectroscopic tool for characterizing the collective rotational response of dipolar species in complex liquid mixtures including aqueous protein solutions. Protein show three anomalous features in their dielectric profile relative to other aqueous mixtures: a dielectric increment of 10-15% over bulk water at low frequencies, an imaginary part of the frequency-dependent dielectric that is bimodal at high protein concentration, and a characteristic dip in the real part of the frequency-dependent dielectric in which the dielectric function of the high concentration protein solution drops precipitously and below the value for the low concentration[6,10,11]. As such, the dielectric dispersion profile measured at room temperature for aqueous protein systems show three distinct time scale signatures: a β–dispersion corresponding to long timescale protein tumbling (~30ns), a γ-dispersion which correspond to the orientational relaxation time due to bulk water (~8.0ps), and two weaker δ-relaxations that has been attributed to a bimodality in the orientational response of water near the protein surface, with relaxation times on the order of ~20-60ps and ~1-10ns.[1-4,7] While the faster δ-dispersion has been argued to arise from water dynamics near the protein surface, the slower δ-dispersion assignment has been more controversial[6-10], although recent simulation evidence supports slowing due to protein-water coupling[6-8] as opposed to hydration and bulk water exchange[10].

In general the peculiarities of protein surface water dynamics exhibits sublinear diffusion for translational motion and stretched exponential behavior for rotational relaxation, similar effects seen in glassy liquids[35]. The conventional wisdom as to the molecular origin of these slow components in the hydration dynamics is thought to be due to trapping of water molecules into crevices and grooves on the topologically rough protein surface[32], although emerging evidence also points to the role of long-lived hydrogen bonding networks near hydrophilic pinning sites, described as energetic

disorder[33]. Our group has presented a number of papers arguing that hydration dynamical anomalies arise from the role of chemical features of the protein surface, not just topology, based on model peptide systems with different side chain chemistries[16-18]. We have studied both the structural organization and dynamics of these solutions using simulation, x-ray scattering[12-14] and quasi-elastic neutron scattering[15-18], enabling us to detect and characterize translational and rotational motions for different hydration layers as a function of concentration, and to do so while contrasting the influence of the amino acid chemistry on the resulting observable. These systems are valuable since we can eliminate the role of topological disorder- for example we see pure linear behavior in the mean square displacement for these peptide systems[35]- allowing us to focus exclusively on the role of chemical heterogeneity[16-18,35], or energy disorder[33]. The question we ask here is whether chemical heterogeneity alone is enough to observe dielectric relaxation anomalies that are seen for protein systems.

In this study we report on molecular dynamics simulations of the frequency-dependent dielectric relaxation spectra in the frequency range of 10^{-4} GHz < ω <10^{4} GHz at room temperature for two aqueous peptide systems at two different concentrations: a model of the hydrophilic backbone, N-acetyl-glycine-methylamide (NAGMA), and an amphiphilic peptide in which the glycine side chain of NAGMA is replaced with the hydrophobic leucine side chain, N-acetyl-leucine-methylamide (NALMA). Furthermore, we perform both a two-component analysis (peptide and water) as well as a three-component analysis (peptide, hydration layer, and outer layers of water) to characterize the populations and timescales of dipolar couplings of the solution constituents. Our results show that the high-concentration NALMA peptide exhibits two well-resolved δ-relaxations and all of the anomalous features of dielectric spectra exhibited by aqueous protein solutions, while the hydrophilic NAGMA peptide does not. While the peptide-water couplings are slowest for the NAGMA and NALMA peptides at all concentrations, the anomalous

dielectric properties of the NALMA solution arises due to an abrupt slowing of the water self- and cross-relaxations upon change of amino acid chemistry from NAGMA to NALMA, which emerges as a second δ-relaxation (~1ns) well-separated in time from the first δ-relaxation (~25ps).

We suggest that frustration from incommensurate hydrogen-bonded water networks around the amphiphilic peptide results in a fast δ-relaxation of hydration layers near the hydrophobic side chain, and a very slow δ-relaxation of hydrogen-bonded waters near the hydrophilic backbone, which do not allow the NALMA solute molecules to reorient on the picosecond timescale of bulk water motions. This explanation is consistent with the idea of "slaving" of residue side chain motions to protein surface water. More speculatively, it suggests that the anomalous dynamics observed from a number of spectroscopies arises at the interface of chemically distinct hydrophilic and hydrophobic domains on a protein surface.

THEORY

A. System and simulation details

Extensive molecular dynamics simulations were performed using an in-house simulation program to study the dielectric properties of aqueous solutions of NALMA and NAGMA at two concentrations. We have also carried out pure water simulations for comparison. We use the AMBER 4.0[19] all-atom force field and potential parameters to model the solutes (NALMA and NAGMA), and the rigid TIP4P-Ew model[20], a re-parameterized version of the standard TIP4P water model for use with Ewald summation techniques, for water molecules. This water model has recently been shown to reproduce many of the bulk water properties (both structural and dynamical) quite well when compared with experiment, including the density maximum at approximately 274 K[20].

All systems were equilibrated in the NPT ensemble at 298K and 1 atm using the Nose-Hoover-Andersen technique[21-23] with the relaxation time constants of 1.0 ps and 0.5 ps for barostat and thermostat, respectively. During this stage, separate Nose-Hoover thermostats were attached to solutes, solvent, and the barostat. The duration of equilibration runs was 0.8-1.2 ns depending on the concentration of the solutions during which the average size of the simulation box was calculated. The production runs then carried out in the NVT ensemble using the Nose-Hoover chain thermostats[24] with the relaxation time constant of 5 ps, setting the box length equal to the average box length from the constant pressure simulations. The velocity Verlet algorithm[25] with a time step of 1 fs was used to integrate the equations of motion.

Three-dimensional cubic periodic boundary conditions were applied and all the electrostatic interactions were calculated using standard Ewald summation with tin-foil boundary conditions. The width of the Gaussian distribution α was set to 0.35 A^{-1} and the reciprocal space sum was truncated with a spherical cutoff of $n_x^2+n_y^2+n_z^2 \leq 105$ where 10 reciprocal space vectors in each direction were used. A potential-based switching function having continuous first and second derivatives was used to smoothly reduce the Lennard-Jones (LJ) and the real space Coulomb interaction energy in the Ewald summation to zero between the cutoffs R_{lower} and R_{upper}. We used molecule-based cutoffs for the water-water interactions with R_{lower} = 9.0Å and R_{upper} = 9.5Å. A long-range correction was also applied to the energy and virial calculations to account for the truncated long-range interactions. For the solute-water and solute-solute interactions, the atom-based cutoffs for the solutes and molecule-based cutoffs for water were used with R_{upper} was set at half of the boxl length and R_{lower} at 0.5Å less than R_{upper}. The intra-molecular geometry of the water molecule (r_{OH} and θ_{HOH}) was constrained by applying the M_SHAKE[26] and M_RATTLE[20] algorithms using an absolute geometric tolerance of 10^{-10}Å. During this stage, coordinates were saved at every 0.02 ps

(20 fs) for subsequent analysis. Further details of the simulation and systems studied are summarized in Table 4.

B. Decomposition into hydration shells

In order to define the solvation environment of the peptides we consider the number of water molecules within the first hydration shell. This quantity may be broken down into two subclasses: 1) the number of water solvating the hydrophilic backbone atoms (O and N atoms), and 2) those that solvate the hydrophobic side chain carbons (in the case of NALMA). The water molecules of the first hydration shell are defined to be within 4.25Å of the peptide heavy atoms as obtained from the first minimum of the radial distribution function. For the hydrophobic side chains the first nearest-neighbor peak of the radial distribution function of water oxygen is around 3.9Å and the corresponding minimum is around 4.25Å. For the backbone atoms, the radial distribution function has two maxima within 4.25Å, the first one is from the waters associated with the backbone via HB around 2.73Å, and the second one belonging to waters which are in the vicinity of the backbone but without an HB at 3.9Å. Therefore in both cases the reasonable cutoff of 4.25Å is chosen. Table 5 summarizes the number count of waters in the first hydration layer and outer hydration layers.

C. Theory of Dielectric Relaxation

Dielectric relaxation measures the frequency-dependent dielectric constant (DC) $\varepsilon(\omega)$ of the system. It is related to the dielectric susceptibility $\chi(\omega)$ by,

$$4\pi\chi(\omega) = \varepsilon(\omega) - 1 \tag{1}$$

The susceptibility $\chi(\omega)$ is related to the total dipole moment time correlation function, $\Phi(t) = \langle \boldsymbol{M}(0)\cdot\boldsymbol{M}(t)\rangle$ according to

$$\chi(\omega) = \chi(\omega = 0) + i\frac{\omega}{3Vk_BT} L\left[\Phi(t)\right] \tag{2}$$

where $\boldsymbol{M}$(t) is the total dipole moment of the simulated system at time t, V is the volume of the system, T is the absolute temperature, and k_B is the Boltzmann constant. L[Φ(t)] is the Fourier-Laplace transform of Φ(t),

$$L\left[\Phi(\tau)\right] = \int_0^\infty \delta\tau e^{i\omega\tau}\Phi(\tau) \tag{3}$$

The real $\chi'(\omega)$ (dielectric dispersion) and imaginary part $\chi''(\omega)$ (dielectric loss) of the complex dielectric susceptibility $\chi(\omega) = \chi'(\omega) + i\,\chi''(\omega)$ are related to each other by,

$$\chi'(\omega) = \chi(\omega = 0) - \frac{\omega}{3Vk_BT}\mathbf{Im}\{L\left[\Phi(t)\right]\} \tag{4}$$

$$\chi''(\omega) = \frac{\omega}{3Vk_BT}\mathbf{Re}\{L\left[\Phi(t)\right]\} \tag{5}$$

where the static susceptibility $\chi_0 = \chi(\omega=0)$ is given by

$$\chi_0 = \chi(\omega = 0) = \frac{\Phi(0)}{3Vk_BT} = \frac{\langle \boldsymbol{M}(0)\cdot\boldsymbol{M}(0)\rangle - \langle \boldsymbol{M}(0)\rangle^2}{3Vk_BT} \tag{6}$$

It is worthwhile to mention that the quantity $\langle \boldsymbol{M}(0)\rangle^2$ vanishes in the limit of long simulation times and can be omitted.

Dielectric component analysis. For an N-component system, when the total dipole moment $\boldsymbol{M}(t)$ of the simulation system is decomposed into sum over the dipole moments of its components $\mathbf{M_i}(t)$, the total dipole moment time correlation function is given by

$$\begin{aligned}\Phi(t) &= \langle M(0)\cdot M(t)\rangle \\ &= \left\langle \sum_{i=1}^{N} M_i(0)\cdot \sum_{j=1}^{N} M_j(t)\right\rangle \\ &= \sum_{i=1}^{N}\sum_{j=1}^{N}\langle M_i(0)\cdot M_j(t)\rangle = \sum_{i=1}^{N}\sum_{j=1}^{N}\Phi_{ij}(t)\end{aligned} \tag{7}$$

where $\Phi_{ij}(t)$ is the time auto ($i=j$) or cross ($i\neq j$) correlation function of the respective component dipole moments $\boldsymbol{M}_i$ and $\boldsymbol{M}_j$.[8-11,27-29] This allows to analyze the contribution of the different terms to the overall frequency-dependent dielectric constant.

The aqueous solutions of peptides studied here are basically two component system (peptide (P) and water (W)) and M(t) can be written as a sum of two component dipole moment, $M(t)=M_P(t)+M_W(t)$, so that the total dipole correlation function becomes

$$\Phi(t) = \Phi_{PP}(t) + 2\Phi_{PW}(t) + \Phi_{WW}(t) \tag{8}$$

Using Eq. (2) and the linearity of the Fourier-Laplace transform, the frequency-dependent dielectric susceptibility of the system thus can be expressed in terms of pair susceptibility χ_{ij} as

$$\chi(\omega) = \chi_{PP}(\omega) + 2\chi_{PW}(\omega) + \chi_{WW}(\omega) \tag{9}$$

It should be noted that a pair susceptibility gives *only* the information about the magnitude of its contribution to the overall susceptibility.

The dynamics of the water molecules near peptides (i.e., water molecules in the first hydration shell) are typically very different compared to all other water molecules in the system. In order to investigate this in detail we decompose the system into three components, peptides (P), first hydration shell water (H), and all other water molecules (W). In this case the total dipole correlation function can be written as,

$$\Phi(t) = \Phi_{PP}(t) + \Phi_{HH}(t) + \Phi_{WW}(t) + 2\Phi_{PH}(t) + 2\Phi_{PW}(t) + 2\Phi_{HW}(t) \tag{10}$$

and the $\chi(\omega)$ can be similarly expressed in terms of the respective pair susceptibility, similar to Eq. (9).

Analysis of the time correlation functions[8]. We have attempted to fit all the component time correlation functions $\Phi_{ij}(t)$ in Eq. (8), as well as the dipole time correlation functions of the whole system $\Phi(t)$, to both a single-exponential

(11)

and a double-exponential function

$$\frac{4\pi}{3Vk_BT}\Phi(t) \approx \Phi^{fit,bi}(t) = A_1 e^{-\frac{t}{\tau_1}} + A_2 e^{-\frac{t}{\tau_2}} \tag{12}$$

with the additional constraint of kinetic mass balance[8]

$$A_2 = \frac{4\pi}{3Vk_BT}\Phi(t=0) - A_1 = 4\pi\chi_0 - A_1 \tag{13}$$

We found that we did not need to fit the data with a stretched exponential function as was done in[9].

RESULTS

The calculated static dielectric constant of TIP4P-EW bulk water of 64 agrees well with what has been reported for TIP4P-EW previously[16] (Table 1), and shows fair agreement with the experimental value at room temperature of 78[30]. The addition of the peptides result in a ~10-20% variation in the calculated static dielectric constant with respect to the homogeneous bulk water liquid (Table 1). There is a dielectric decrement for NAGMA at all concentrations. By contrast the low concentration NALMA solution has a dielectric constant below bulk water, but exhibits a dielectric increment of ~15% relative to bulk water for the high concentration NALMA solution. We note that the dielectric increment for the NALMA peptide is unusual since it is not zwitterionic like previous peptide solute studies[9].

Furthermore, it is only the high concentration amphiphilic NALMA solution that shows two additional unusual features of dielectric relaxation behavior for protein solutions: the characteristic dip in the real part of the frequency-dependent dielectric function in which the high concentration solution drops precipitously and below the value for the low concentration (Figure 1a), and an imaginary part of the frequency-dependent dielectric spectra that is bimodal at high concentration (Figure 1b). The low concentration NALMA solution, and the purely polar NAGMA peptide solution at any concentration, shows no such anomalous behavior (Figure 1).

Table 1 also reports the single and double exponential fit to the total dipole moment correlation function for simulated TIP4P-EW bulk water yielding a relaxation timescale of 11ps, whereas the experimental value is 8ps[1-6]. The low concentration NALMA and NAGMA peptide at both concentrations show evidence of two rotational relaxation timescales, with roughly 80-85% of the signal arising from bulk-like (simulation) water timescales of ~11-16ps, while the remaining signal yields a slower motion of 51ps for 1M NAGMA, 88ps for 0.5M NALMA, and 123ps for 3M NAGMA. The high concentration NALMA peptide also shows evidence of two rotational relaxation timescales of 19ps well separated from an especially slow motion of 719ps making up almost half of the signal.

To better understand the origin of the bimodality in the dielectric relaxation spectra, we dissect the dipole correlation function into constituent components of protein-protein (PP), protein-water (PW), and water-water (WW) correlations. Table 2 reports the single and/or double exponential fits to the components of the dipole moment correlation function for all peptide solutions; we ignore amplitudes of less than or equal to 1% in our analysis. For the low concentration peptides the dominant component is confirmed to arise from almost purely WW correlations that are essentially identical to bulk-like simulated water timescales. The remaining ~15% of the signal is due to lower frequency components arising from water self-correlations,

water-peptide cross-correlations, and peptide self-correlations in order of decreasing importance, all with an (average) long timescale corresponding to ~50ps for NAGMA and ~100ps for NALMA. At this level of decomposition, the two peptides at low concentration look very similar, with their amino acid chemistries not strongly differentiated in qualitative features of the amplitudes or timescales of constituent couplings, as seen in both the real and imaginary components of the frequency dependent dielectric function shown in Figure 2.

By contrast, the bimodality in the timescales of the fit to the total dipole correlation function for the high concentration NAGMA and NALMA peptides arises from both fast and slow timescale contributions from all components. This is apparent in both the real and imaginary components of the dielectric function in Figure 3, in which we see that all solution constituents and their couplings contribute to the enhancement of the lower frequency region for the high concentration peptides. For NAGMA we see a fast reorientation timescale of 12-32ps making up close to 80% of the total amplitude, while the remaining signal is comprised of a slow component dominated by WW and PW dipolar couplings with a timescale of ~100ps (Table 2). For NAGMA and the low concentration solutions, which show no anomalous dielectric behavior, no dipolar coupling component exhibits the slow δ-relaxation of ~1ns observed in protein systems.[1-4, 7]

For NALMA, which shows all of the anomalous dielectric behavior similar to proteins, almost half the amplitude arises from slow reorientations of water self-correlations, water-peptide cross-correlations, and peptide self-correlations in a ratio proportion of 13%:20%:10%, and all exhibit a relaxation time of ~1ns that is identified as the slow δ-relaxation for aqueous protein systems[1-4, 7]. This is also apparent in both the real and imaginary components of the dielectric function in Figure 3, in which we see a far greater shift to lower frequency for the NALMA peptide relative to NAGMA.

We do a final level of analysis to differentiate the peptide, the first hydration layer (which we label H), and the outer hydration layers (which we label W), to determine whether the dielectric anomalies and the emergence of two δ-relaxations for NALMA arise from the hydration layer immediate to the peptide surface. This level of decomposition is much more ambiguous due to the subjective definition of the first hydration layer, and error prone due to the constant exchange of water molecules between hydration layers, and the quality of single or double exponential fits is less good than the two component analysis. Again, we eliminate contributions of amplitudes of less than or equal to 1%.

Under this analysis, the low concentration peptide solutions, and the high concentration NAGMA peptide, show strong spatial heterogeneity in the water dynamics relative to the two-component analysis (Table 3). These three solutions show non-trivial amplitudes of HH and/or WW dipolar couplings with timescales faster than bulk water, ~40-60% from bulk-like timescales, ~30% of slow water timescales of ~20-25ps, with the 1M NALMA and 3M NAGMA also exhibiting additional slow components of ~80-100ps from water self-correlations. By contrast, there is less spatial heterogeneity in the water dynamics for the high concentration NALMA solution, with ~20% from bulk-like timescales, ~36% of slow water timescales of ~20-27ps arising from HH and HW constituents, and ~11% of a slow component of ~650-900ps from all hydration layers and their couplings (Table 3).

Based on these progressive series of dipolar couplings analysis, we find a fast δ-relaxation that emanates from the hydration layer, i.e. primarily HH and HW correlations with a timescale of ~25ps. for all peptide solutions. However, the dielectric anomalies for the high concentration NALMA stem from the emergence of a second and much lower frequency δ-relaxation process of strong protein dipolar couplings to all constituents, accompanied by a slowing of the structural

relaxation in all water layers, giving rise to timescales close to ~1ns that are strongly separated from the picosecond timescales of the first δ-relaxation.

DISCUSSION AND CONCLUSIONS

There has been significant disagreement in the literature about the role of hydration water in explaining anomalous dielectric relaxation behavior and the molecular origin of multimodal δ-relaxations observed for protein solutions. There is overall agreement that the high frequency δ-relaxation corresponding to 20-60ps arises from the hydration layer[6-10], and this work continues to support that conclusion. What remains controversial is the origin of a second δ-relaxation on the nanosecond timescale[6-10]. Nandi and coworkers[4-7,10] have advanced a microscopic phenomenological theory that reproduces the anomalous trends observed for protein solutions, that emphasizes the dominance of the hydration and bulk water cross-correlation as the origin of relaxation anomalies. Boresch and co-workers[9] using molecular dynamics simulations of ubiquitin in water conclude that the slower δ-relaxation arises exclusively from protein-water cross-terms. Oleinikova and co-workers[6] found three δ-dispersions in their dielectric relaxation spectra of ribonuclease-A, but attribute the protein-water relaxations as the origin of the lowest frequency δ-dispersion, and suggest that fluctuations of polar side chains may drive the intermediate frequency δ-dispersion on a sub-nanosecond time scale.

What we find for the peptide systems is that the high concentration NALMA peptide shows the same dielectric anomalies of aqueous protein solutions while the other peptide solutions do not. While the peptide-water couplings are certainly the slowest for the NAGMA and NALMA peptides at all concentrations, the anomalous dielectric properties of the NALMA solution arises due to an abrupt slowing of the water self- and cross-relaxations upon change of amino acid chemistry from

NAGMA to NALMA, which emerges as a second δ-relaxation (~1ns) well-separated in time from the first δ-relaxation (~25ps).

No one as far as we are aware has focused on whether the dielectric anomalies and δ-relaxations observed for protein solutions arise from some feature of the protein surface chemistry. In fact NMR studies have asserted that there is no correlation with water dynamical anomalies and amino acid chemistry, and that the longer δ-relaxation has no connection to water dynamics at all[32], although this broad assertion remains controversial given the differences in spectroscopies and their information content[16]. The obvious question is to how to interpret the dynamical features of high concentrations of peptides in water with the corresponding relaxation dynamics of aqueous protein systems. The significant differences in size between the peptides studied here and large globular proteins means that the β–relaxations of protein solutions[1-6] are not represented in these peptide solutions. We have also eliminated the effects due to topological disorder since the mean square displacements of water near small peptides show no sublinear trends that are found from extended protein surfaces. The high concentration NAGMA solution indicates that this is not simply a confinement effect.

However, what we believe is similar is that these peptide studies probe the constituent relaxations at the resolution of amino acids on the protein surface, and that the chemical nature of peptide can induce differences in energetic disorder which has been seen recently for simulations on lysozyme. Our DR simulations that exhibit anomalous dielectric behavior for high concentrations of NALMA and not NAGMA are consistent with our quasi-elastic neutron scattering experiments[15-18] that show anomalous single particle diffusion behavior for water in the NALMA solution, which does not exist for aqueous NAGMA. We have shown from related molecular dynamics and QENS studies that hydrogen-bonded networks in the two distinct chemical regions of the NALMA peptide

promote a very slow δ-relaxation of long-lived hydrogen-bonded waters near the backbone, while the fast δ-relaxation is dominated by water exchange within and between hydration and outer water layers near the hydrophobic side chain[15-18]. This is consistent with the recent lysozyme study which found that rotational relaxations were *faster* than bulk water when electrostatic interactions were turned off[33]. In our view, the anomalies from both spectroscopies are related to frustrated motions of these incommensurate water networks, that in turn do not allow the NALMA solute molecules to reorient or translationally diffuse on the picosecond timescale of bulk water motions. Thus the spatial heterogeneity in the water dynamics measured by QENS shares the same molecular origin as the multimodal features of the DR spectra that measures both peptide and water relaxations. This evidence is consistent with the idea of "slaving" of residue side chain motions to protein surface water[31].

While highly speculative, we suggest that it is the interface of chemically distinct domains on the protein surface that is the molecular origin of the multimodal δ-relaxations and hence the dielectric or quasi-elastic anomalies of aqueous protein solutions. Since heterogeneous chemical surfaces are a structural feature of all globular proteins, it explains why anomalous DR signatures and δ-relaxations can be categorized into mean values observed for all proteins. However the spread in these dynamical values may in fact arise from differences in the size and distribution of hydrophobic and hydrophilic domains among different proteins. Therefore DR spectra measured for unusually hydrophobic proteins such as crambin vs. strongly hydrophilic surfaces may explain the extremes in timescales and anomalies among particular proteins.

Acknowledgments. We gratefully acknowledge the support of the Department of Energy, Condensed Phase and Interfacial Molecular Science Program, DE-AC02-05CH11231.

References.

1. Grant, E. H.; Sheppard, R. J.; South, P. G. *Dielectric behavior of biological molecules in solutions*; Clarendon: Oxford, 1978.

2. Dachwitz, E.; Parak, F.; Stockhausen, M. *Ber. Bunsen-Ges. Phys. Chm*. **1989**, *93*, 1454-1458.

3. Pethig, R. *Annu Rev Phys Chem*. **1992**, *43*, 177-205.

4. Nandi, N.; Bhattacharyya, K.; Bagchi, B. *Chemical Reviews* **2000**, *100*, 2013-2046.

5. Knocks, A.; Weingartner, H. *J. Phys. Chem. B* **2001**, *105*, 3635-3638.

6. Oleinikova, A.; Sasisanker, P.; Weingartner, H. *J. Phys. Chem. B* **2004**, *108*, 8467-8474.

7. Nandi, N.; Bagchi, B. *J. Phys. Chem. B* **1997**, *101*, 10954-10961.

8. Boresch, S.; Hochtl, P.; Steinhauser, O. *J. Phys. Chem. B* **2000**, *104*, 8743-8752.

9. Boresch, S.; Willensdorfer, M.; Steinhauser, O. *J. Phys. Chem. B* **2004**, *120*, 3333-3347.

10. Nandi, N.; Bagchi, B. *J. Phys. Chem. A* **1998**, *102*, 8217-8221.

11. Pethig, R. *Protein Solvent Interactions*; Gregory, R.B., Ed.; Marcel Dekker: New York, **1995**; Chapter 4.

12. Hura, G.; Sorenson, J. M.; Glaeser, R. M.; Head-Gordon, T. *Perspectives in Drug Discovery & Design* **1999**, 17, 97-118.

13. Pertsemlidis, A.; Soper, A. K.; Sorenson, J. M.; Head-Gordon, T. *Proc Natl Acad Sci USA* **1999**, *96*, 481-486.

14. Sorenson, J. M.; Hura, G.; Soper, A. K.; Pertsemlidis, A.; Head-Gordon, T. *J. Phys. Chem. B* **1999**, *103*, 5413-5426.

15. Malardier-Jugroot, C.; Head-Gordon, T. *Phys. Chem. Chem. Phys.* **2007**, *9*, *1962-1971*.

16. Russo, D.; Murarka, R. K.; Copley, J. R. D.; Head-Gordon, T. *J. Phys. Chem. B* **2005**, *109*, 12966-12975.

17. Russo, D.; Murarka, R. K.; Hura, G.; Verschell, E. R.; Copley, J. R. D.; Head-Gordon, T. *J. Phys. Chem. B* **2004**, *108*, 19885-19893.

18. Russo, D.; Hura, G.; Head-Gordon, T. *Biophys. J.* **2004**, *86*, 1852-1862.

19. Cornell, W. D.; Cieplak, P.; Bayly, C. I.; Gould, I. R.; Merz, K. M.; Ferguson, D. M.; Spellmeyer, D. C.; Fox, T.; Caldwell, J. W.; Kollman, P. A. *J. Am. Chem. Soc.* **1995**, *117*, 5179-5197.

20. Horn, H. W.; Swope, W.C.; Pitera, J. W.; Madura, J. D.; Dick, T. J.; Hura, G.; Head-Gordon, T. *J. Chem. Phys.* **2004**, *120*, 9665-9678.

21. Andersen, H. C. *J. Chem. Phys.* **1980**, *72*, 2384-2393.

22. Nose, S. *Mol. Phys.* **1984**, *52*, 255-268.

23. Hoover, W. G. *Phys. Rev. A* **1985**, *31*, 1695-1697.

24. Martyna, G. J.; Tuckerman, M. E.; Klein, M. L. *J. Chem. Phys.* **1992**, *97*, 2635-2643.

25. Anderson, H. C. *J. Comp. Phys.* **1983**, *52*, 24-34.

26. Kraeutler, V.; van Gunsteren, W. F.; Huenenberger, P. H. *J. Comput. Chem.* **2001**, *22*, 501-508.

27. Zwanzig, R. *Annu. Rev. Phys. Chem.* **1975**, *16*, 67-102.

28. Titulaer, U. M.; Deutch, J. M. *J. Chem. Phys.* **1974**, *60*, 1502-1513.

29. Williams, G. *Chem. Rev.* **1972**, *72*, 55-69.

30. Kell, G. S. *J. Chem. Eng. Data* **1975**, *20*, 97-105.

31. Fenimore, P. W.; Frauenfelder, H.; McMahon, B. H.; Parak, F. G. *Proc Natl Acad Sci USA* **2002**, *99*, 16047-16051.

32. Halle, B. *Philos Trans R Soc Lond B Biol Sci* **2004**, *359*, 1207.

33. Pizzitutti, F.; Marchi, M.; Sterpone, F.; Rossky, P. J. *J. Phys. Chem. B* **2007**, *111*, 7584 -7590, 2007.

34. Murakra, R. K.; Head-Gordon, T. . *J. Chem. Phys.* **2007**, *126*, 215101-215109.

35. Bizzarri, A. R.; Cannistraro, S. J. *J. Phys. Chem. B* **2002**, *106*, 6617-.

TABLE 1. *Single and double exponential fits of the overall static and dynamic dielectric properties of the NALMA and NAGMA solutions and pure WATER.*

Conc./Solute	$4\pi\chi_0 \pm \sigma$	A_1	τ_1	A_2	τ_2
Pure WATER	63.54±1.14	63.54	10.8	….	……
NAGMA/1.0M	61.47±1.62	51.57	11.5	9.90	51.5
NALMA/0.5M	57.46±1.42	49.61	11.1	7.85	88.0
NAGMA/3.0M	50.58±0.75	39.80	16.2	10.78	123.0
NALMA/2.0M	69.14±2.11	38.56	18.8	30.58	719.0

TABLE 2. *Single and double exponential fits of the peptide and water components of the dynamic dielectric properties of the NALMA and NAGMA solutions.*

	WW				2xPW				PP			
Conc./Solute	A_1	τ_1	A_2	τ_2	A_1	τ_1	A_2	τ_2	A_1	τ_1	A_2	τ_2
NAGMA/1.0M	50.6	11.6	5.6	53.0			3.4	40.0	0.8	11.3	1.0	66.5
NALMA/0.5M	50.7	11.4	3.7	120.0			2.1	97.4	0.1	2.8	0.9	91.0
NAGMA/3.0M	35.6	15.4	4.7	111.4	0.8	12.2	5.3	92.0	2.8	32.0	1.4	198.0
NALMA/2.0M	37.3	18.6	9.2	688.0	1.1	74.2	13.8	819.0	0.6	10.3	7.1	748.0

TABLE 3. Single and Double exponential fits of further decomposition of peptide and water components of the dynamic dielectric properties of the NALMA and NAGMA solutions.

Conc./Solute	WW				HH				2xHW			
	A_1	τ_1	A_2	τ_2	A_1	τ_1	A_2	τ_2	A_1	τ_1	A_2	τ_2
NAGMA/1.0M	26.0	12.7	4.5	1.3	7.0	6.0	4.6	26.0	14.1	20.0		
NALMA/0.5M	33.8	10.0	1.8	97.0	3.2	3.0	5.0	21.5	10.5	22.3		
NAGMA/3.0M	4.3	19.0	3.2	2.0	19.0	13.0	4.5	79.2	9.4	25.0		
NALMA/2.0M	13.7	11.0	1.2	664.0	14.0	19.0	4.3	656.0	11.0	27.0	2.0	907.0
	$2 \times$ PW				$2 \times$ PH				PP			
	A_1	τ_1	A_2	τ_2	A_1	τ_1	A_2	τ_2	A_1	τ_1	A_2	τ_2
NAGMA/1.0M			1.6	36.0	1.9	42.4			0.8	11.3	1.0	66.5
NALMA/0.5M			1.1	103.0			1.0	99.0			0.9	91.0
NAGMA/3.0M	0.4	13.2	0.8	127.0	0.5	12.9	4.4	88.7	2.8	32.0	1.4	198.0
NALMA/2.0M	0.6	145.0	3.9	1006.0	0.6	64.8	9.8	760.0	0.6	10.3	7.1	748.0

TABLE 4. Molecular dynamics simulation details of bulk water and aqueous peptide solutions.

System	**Number of simulations**	**Number of peptides**	**Number of waters**	**Average box length**	**Length of each simulation**
Water	2		512	24.8725769	6 ns
NAGMA/1.0M	4	8	440	24.4890402	6 ns
NAGMA/3.0M	3	24	432	25.7226113	18 ns
NALMA/0.5M	4	5	462	24.8382851	6 ns
NALMA/2.0M	3	15	362	24.7885838	21 ns

TABLE 5. *Average number of waters in the first hydration shell (N_H) and remaining waters (N_W)*

System	N_H	N_H/N_{Solute}	N_W	Total # of Water (N_T)
NAGMA/1.0M	145.6	18.2	294.4	440
NAGMA/3.0M	309.6	12.9	122.4	432
NALMA/0.5M	112.0	22.4	350.0	462
NALMA/2.0M	190.5	12.7	171.5	362

Figure Captions

Figure 1. *A comparison of the total frequency-dependent dielectric response for the four aqueous peptide solutions and bulk water using molecular dynamics simulation.* (a) real part of dielectric function and (b) imaginary part of dielectric function.

Figure 2. *Molecular dynamics simulations of the frequency-dependent dielectric response for the aqueous peptide solution at low concentration.* (a) real part of dielectric function for 1.0M NAGMA, (b) real part of dielectric function for 0.5M NALMA, (c) imaginaty part of dielectric function for 1.0M NAGMA, (b) imaginary part of dielectric function for 0.5M NALMA.

Figure 3. *Molecular dynamics simulations of the frequency-dependent dielectric response for the aqueous peptide solution at high concentration.* (a) real part of dielectric function for 3.0M NAGMA, (b) real part of dielectric function for 2.0M NALMA, (c) imaginary part of dielectric function for 3.0M NAGMA, (b) imaginary part of dielectric function for 2.0M NALMA.

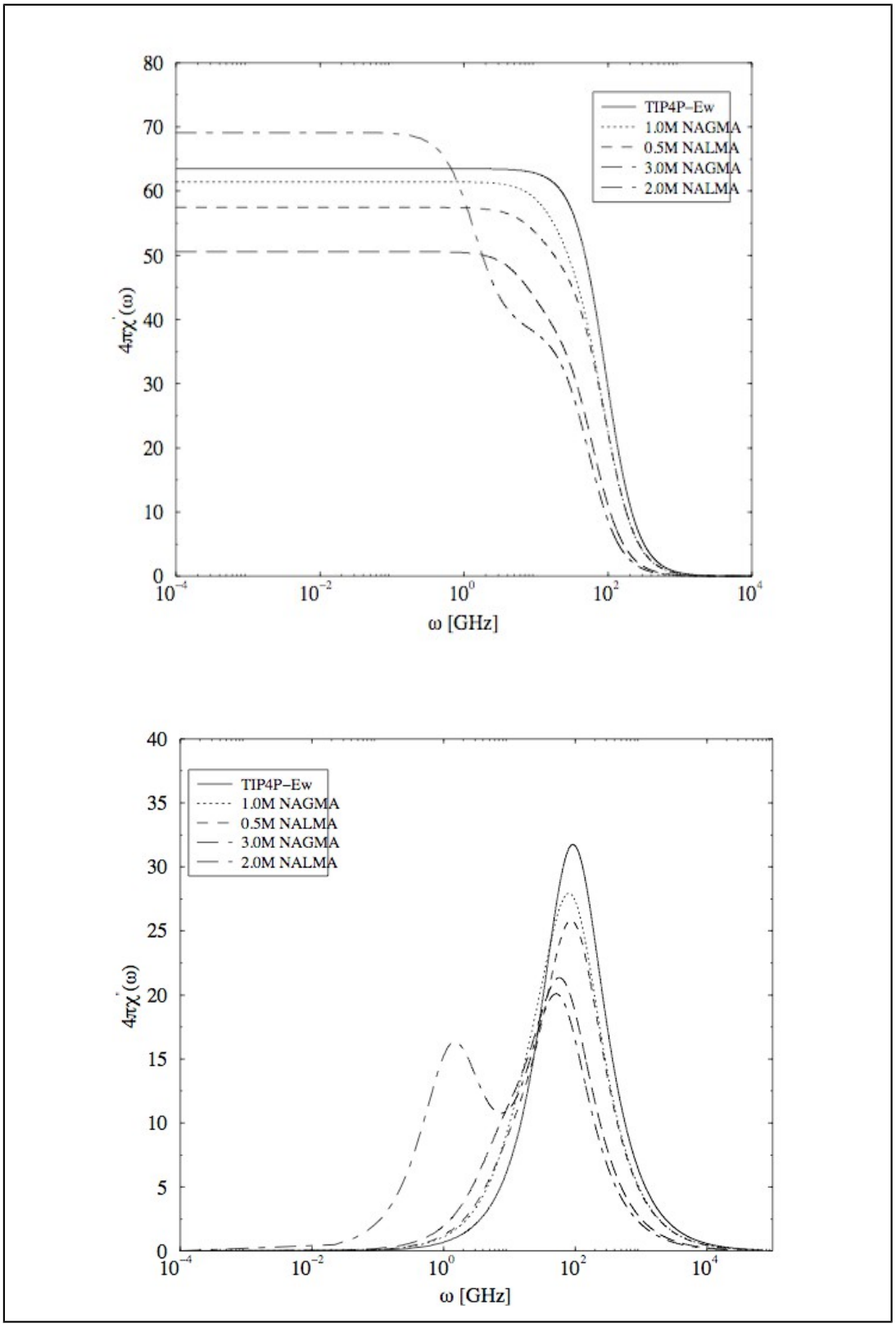

Figure 1: Murarka and Head-Gordon

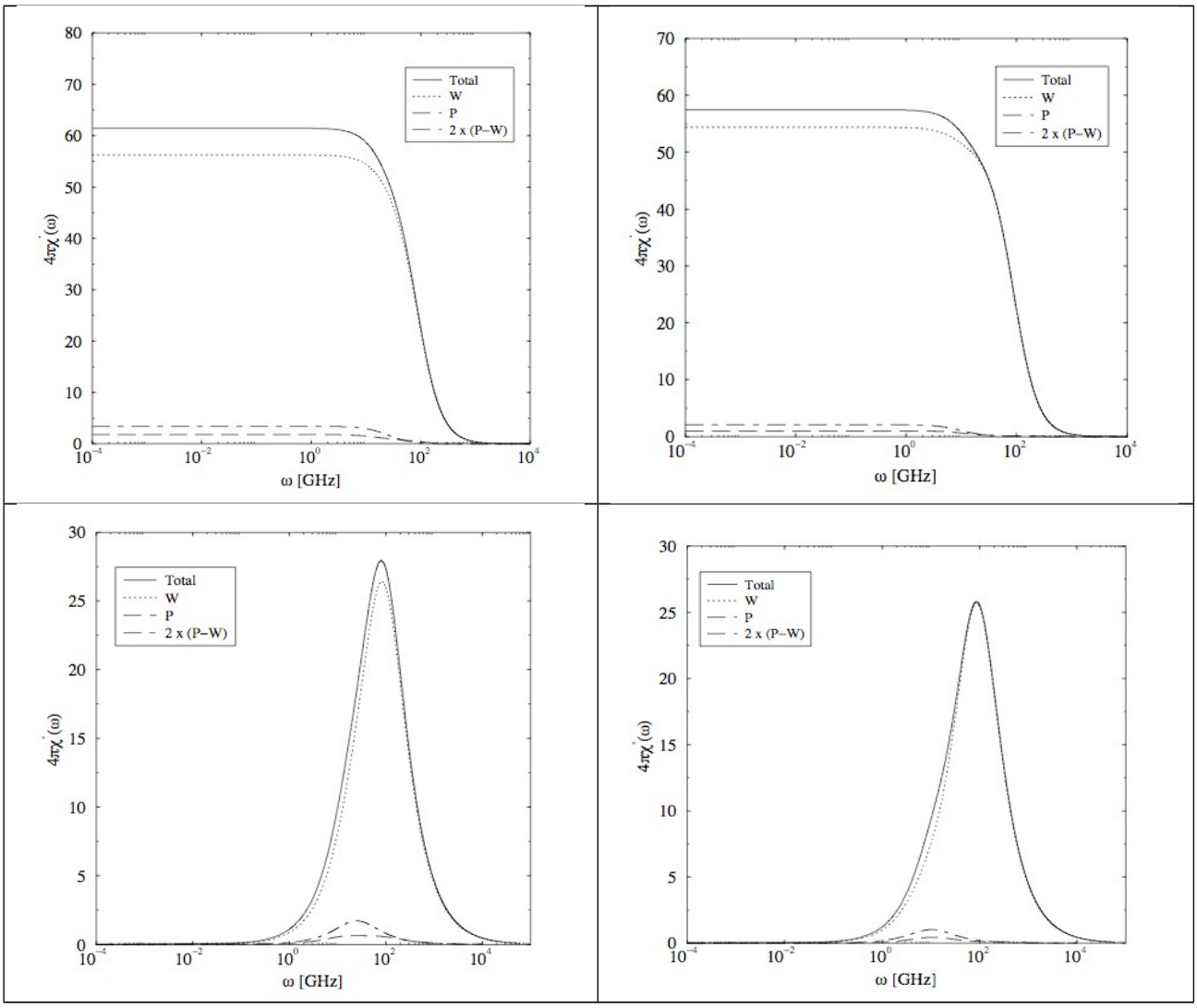

Figure 2: Murarka and Head-Gordon

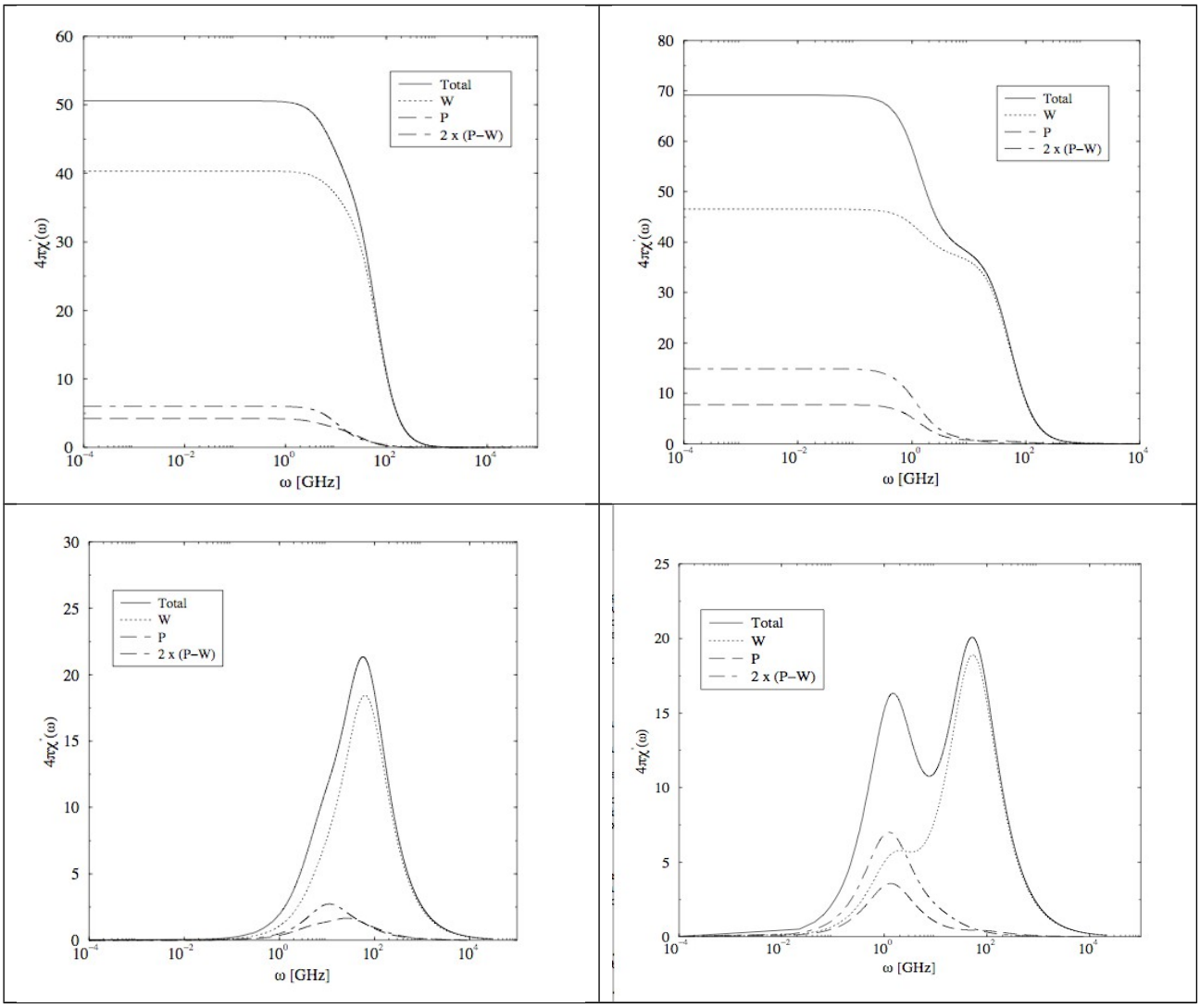

Figure 3: Murarka and Head-Gordon